Initial results of a study into the estimation of the development of frequency lock-in for offshore structures subjected to ice loading

Hendrikse, Hayo; Seidel, Marc; Metrikine, Andrei; Loset, Sveinung

Publication date
2017

Document Version
Final published version

Published in
Proceedings of the 24th International Conference on Port and Ocean Engineering under Arctic Conditions

Citation (APA)
Hendrikse, H., Seidel, M., Metrikine, A., & Loset, S. (2017). Initial results of a study into the estimation of the development of frequency lock-in for offshore structures subjected to ice loading. In *Proceedings of the 24th International Conference on Port and Ocean Engineering under Arctic Conditions: June 11-16, 2017, Busan, Korea* Article POAC17-187

POAC'17
Busan, KOREA

Proceedings of the 24th International Conference on
Port and Ocean Engineering under Arctic Conditions
June 11-16, 2017, Busan, Korea

Initial results of a study into the estimation of the development of frequency lock-in for offshore structures subjected to ice loading

Hayo Hendrikse[1,4], Marc Seidel[2], Andrei Metrikine[1,4], Sveinung Løset[3,4]
[1] Delft University of Technology, Delft, the Netherlands
[2] Siemens Wind Power GmbH & Co. KG, Germany
[3] NTNU, Trondheim, Norway
[4] Sustainable Arctic Marine and Coastal Technology (SAMCoT), Trondheim, Norway

ABSTRACT

Ice-induced vibrations have to be considered in design of vertically sided offshore structures subjected to loading by sea ice, such as offshore wind turbines and oil- and gas platforms. The interaction between ice and structure may result in high global peak loads and the occurring structural vibrations can contribute significantly to the overall fatigue of the structure. A regime of particular interest is the frequency lock-in regime in which the interaction causes the structure to oscillate at high amplitude with a frequency close to one of its natural frequencies. Assessment of frequency lock-in in the design phase can be done based on simple approaches once for given ice conditions the natural modes to experience frequency lock-in and the range of ice drift velocities for which lock-in develops are known. Determining those modes and velocities is however challenging due to the nonlinear nature of the interaction between ice and structure and limited available reference data. In this paper two methods are applied to determine the structural modes and ice drift velocities required as an input for simplified design approaches. The first method is the application of design standards and estimation formulas available from literature. The second method is the application of a recently developed numerical model for simulation of the interaction. The methods are applied to two existing structures which have experienced frequency lock-in and an offshore wind turbine designed to be employed at a location with mild ice conditions. Results show that the estimation formulas do not match with full-scale observations of the existing structures and can therefore not be applied to obtain input for the simplified design approaches. The second method shows to give simulation results consistent with the full-scale observations. Application to the offshore wind turbine reveals that it is most susceptible to frequency lock-in in the second mode.

KEY WORDS: Ice-induced vibrations; frequency lock-in; offshore wind; structural design.

INTRODUCTION

Ice-induced vibrations of offshore structures in cold regions pose a design challenge which has been studied for decades. The Cook Inlet observations (Peyton, 1968, Blenkarn, 1970), the Molikpaq 'incident' in the eighties (Jefferies and Wright, 1988), and the large experimental and full-scale campaigns in the nineties (Saeki et al., 1996; Schwarz and

Jochmann, 2001) being of major importance to the developments. Recently the topic has gained new interest with respect to projected offshore wind developments at locations in the Baltic Sea and Bohai Sea.

Three regimes of interaction are typically distinguished (ISO19906, 2010), being intermittent crushing, frequency lock-in, and continuous brittle crushing. The frequency lock-in regime is of particular interest with respect to offshore wind developments. The typical support structures consisting of a tower and monopile result in low natural frequencies of the first modes and relatively low damping ratios which makes the structures theoretically very susceptible to frequency lock-in.

During frequency lock-in the structural oscillation shows some typical characteristics which allow for a simplified analysis of the impact for extreme (ULS) and fatigue (FLS) conditions (see for measured signals e.g. Huang et al., 2007; Izumiyama et al., 1994; Singh et al., 1990; Toyama et al., 1983). Typical structural displacement, structural velocity, and ice load signals illustrating those characteristics are shown in Figure 1. The signal is close to harmonic with a frequency often slightly below the natural frequency of the mode of the structure in which lock-in has developed. The deviation from the harmonic signal generally occurs at the time moment when the structure reverses its direction of motion and starts to move towards the ice as seen at the moments the velocity of the structure changes from positive to negative in Figure 1. The velocity amplitude of structural motion is found to be in the range of 1.0 up to 1.5 times the ice velocity in experiments and full-scale data (Toyama et al., 1983). Using these observations the oscillation of the structure during frequency lock-in can be approximated by:

$$u_s(t) = \frac{F_{mean}}{K_s} + \frac{\beta v_{ice}}{\omega_n} \sin(\omega_n t) \tag{1}$$

, with u_s the structural displacement at the ice action point [m], F_{mean} the mean global ice load [N], K_s the structural stiffness at the ice action point [N/m], β a factor between 1.0 and 1.5 [-], v_{ice} the ice drift velocity [m/s], ω_n the natural frequency of the mode in which frequency lock-in develops [rad/s], and time t [s].

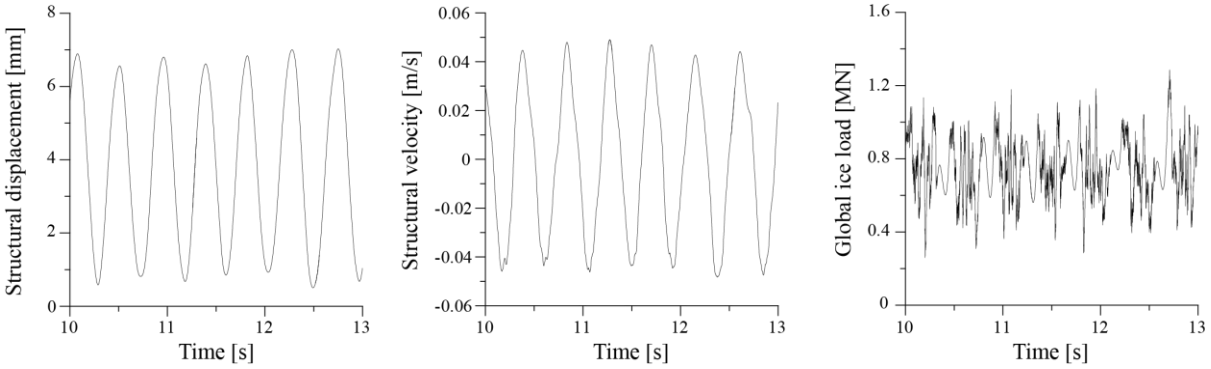

Figure 1. Typical (simulated) structural displacement, structural velocity, and global ice load during frequency lock-in of a structure with a natural frequency of 2.32 Hz at an ice drift velocity of 0.04 m/s.

The impact on design for ULS and FLS conditions can be verified by applying an oscillation pattern of the ice action point of the structure according to Eq. (1) in detailed numerical

models of the structure. In order to do so it is required to know the global ice load, the modes to consider, and the ice drift velocities for which frequency lock-in can develop for relevant ice conditions. Note that this approach is valid for situations where other external loads are not causing significant structural motion. When significant interaction of the structure with wind or currents takes place, such that the structural motion is altered during interaction with the ice only a fully coupled numerical simulation of the interaction can be used to assess the development of frequency lock-in. It should additionally be checked whether limiting mechanisms such as ice buckling are expected to occur that would eliminate the possibility for frequency lock-in to develop.

In this paper we look into the challenge of estimating the structural modes and ice drift velocities for which frequency lock-in can develop in given ice conditions. Two methods are applied: the first method is based on ISO19906 (2010) and estimation formulas available in literature, and the second method incorporates a recently developed numerical model for simulation of the interaction (Hendrikse and Metrikine, 2016). Both methods are applied to two existing structures which have experienced frequency lock-in in order to evaluate their applicability. These structures are the Norströmsgrund lighthouse located in the Gulf of Bothnia and the Monopod MDP-1 located in the Bohai Sea. The methods are also applied to study an offshore wind turbine on monopile foundation designed for southern Baltic Sea conditions.

In Section 2 the relevant structural and ice parameters of the three structures are presented which are used as input for the analysis in this paper. In Section 3 an estimate of the modes in which frequency lock-in can develop and the velocity range over which it develops on the basis of design standards and estimation formulas from literature is presented. In Section 4 the same quantities are obtained from simulations with a recently developed numerical model. In Section 5 the results are discussed and in Section 6 the conclusions are presented.

STRUCTURES CONSIDERED IN THE ANALYSIS

For our analysis we take into consideration the first four modes of an offshore wind turbine on a cylindrical monopile foundation designed for southern Baltic Sea conditions. Higher modes are not included here as the analysis serves as an example, but for a real design all relevant modes have to be included. The modal properties of the first four modes are given in Table 1. Both the generalized mass M_g for eigenvectors scaled to one at maximum deflection, and the oscillating mass M_s used in a single-degree-of-freedom (scaled to modal deflection at the ice action point) representation are given. Φ is the modal amplitude at the ice action point. The foundation has a diameter d of 6 m at the ice action point and the structure is envisaged to be employed at a location with a 50-year ice thickness h_{50} of 0.4 m.

Table 1. Modal properties of first four modes of the studied offshore wind turbine.

Mode	f_n [Hz]	ζ_n [-]	M_s [t]	Φ [-]	M_g [t]
1	0.226	0.01	$2.9 \cdot 10^4$	0.147	615
2	0.626	0.01	$3.9 \cdot 10^3$	0.854	2850
3	1.546	0.01	$9.8 \cdot 10^6$	0.008	624
4	1.709	0.01	$1.5 \cdot 10^5$	0.059	513

We also consider two existing structures being the Norströmsgrund lighthouse located in the Gulf of Bothnia and the Monopod MDP-1 located in the Bohai Sea. For both structures only the first mode is considered as frequency lock-in has occurred mainly in mode one. It is again noted that in a real design scenario more modes should be included in the analysis. Table 2 shows the properties of the structures used in the analysis based on Guo (2012). Upper bound measured values for the ice thickness (*h)* and the reported range of velocities (v_{fli}) where frequency lock-in occurred are given (Yue et al., 2002; Ice Induced Vibrations JIP, 2011).

Table 2. Parameters used in analysis of the Norströmsgrund lighthouse and MDP-1 monopod.

Structure	f_n [Hz]	ζ [-]	M_s [t]	d [m]	h [m]	v_{fli} [m/s]
Norströmsgrund lighthouse	2.6	0.02	$3.5 \cdot 10^3$	7.5	1	0.02 – 0.12
Monopod MDP-1	2.32	0.03	$9.25 \cdot 10^2$	1.78	0.5	0.02 – 0.04

Estimates of the global ice load are required for the numerical simulations and are obtained based on formula A.8-21 in ISO19906 (2010):

$$F_{iso} = hdC_R \left(h\right)^{-0.5+h/5} \left(\frac{w}{h}\right)^{-0.16} \tag{2}$$

, where F_{iso} is an estimate of the maximum load during continuous brittle crushing [N], and w is the structure width or diameter [m]. Results for different C_R values are given in Table 3. We have chosen the C_R values to represent different estimations of ice load levels for continuous crushing based on ISO19906 and a discussion on ice load estimation by Gravesen and Kärnä (2009). The load levels presented in Table 3 are used as reference for input in the numerical simulations described in Section 4. It is noted that these estimates represent maxima during continuous brittle crushing which is a different interaction regime than frequency lock-in. During continuous brittle crushing the ice load is not affected by the structural motion.

Table 3. Maximum global load during continuous brittle crushing based on Eq. (2).

Structure	C_R = 1.0 MPa	C_R = 1.4 MPa	C_R = 1.8 MPa
Norströmsgrund lighthouse	$5.43 \cdot 10^6$ N	$7.61 \cdot 10^6$ N	$9.78 \cdot 10^6$ N
Monopod MDP-1	$9.58 \cdot 10^5$ N	$1.34 \cdot 10^6$ N	$1.73 \cdot 10^6$ N
Offshore wind turbine	$2.29 \cdot 10^6$ N	$3.20 \cdot 10^6$ N	$4.12 \cdot 10^6$ N

APPLICATION OF DESIGN STANDARDS AND ANALYTICAL FORMULAS

The applicable design standards IEC61400-3 and ISO19906 are soon to be revised, but the analysis method for frequency lock-in is not expected to change significantly from the method presented in the current version of ISO19906 (2010). We will therefore follow the approach presented in the current version of ISO19906 for our analysis.

The susceptibility of different modes of oscillation of a structure to frequency lock-in can be determined based on formula A.8-69 from ISO19906 (2010):

$$\zeta_n \geq \frac{\phi_{nc}^2}{4\pi f_n M_n} h\theta \tag{3}$$

, with ζ_n the damping ratio as a fraction of critical of mode n [-], f_n the natural frequency of mode n [Hz], M_n the generalized mass for eigenvectors scaled to one at the maximum deflection of mode n [kg], h the ice thickness [m], Φ_{nc} the modal amplitude at the ice action point of mode n [m], and θ an empirical coefficient equal to $40 \cdot 10^6$ [kg/ms]. Results of application of Eq. (3) to the structures considered are shown in Table 4. Frequency lock-in is expected for the lighthouse and monopod in mode one, and for the offshore wind turbine in mode one and two for the specified ice conditions.

Table 4. Susceptibility of modes based on Eq. (2).

Structure	ζ [-]	RHS Eq. (2)	FLI
Norströmsgrund lighthouse	0.02	0.35	Yes
Monopod MDP-1	0.03	0.74	Yes
OWT mode 1	0.01	0.19	Yes
OWT mode 2	0.01	0.52	Yes
OWT mode 3	0.01	0.00008	No
OWT mode 4	0.01	0.0051	No

The second step is to find the maximum ice drift velocity ($v_{maxfli,n}$), or the range of velocities (v_{fli}), at which frequency lock-in can develop for the identified susceptible modes. Several approaches have been proposed in literature to estimate the maximum velocity at which frequency lock-in can develop. ISO19906 (2010) gives formula (A.8-71):

$$v_{maxfli,n} = 0.06 f_n \tag{4}$$

Guo (2013) suggests a dependence on the transitional strain rate between ductile and brittle ice behavior $\dot{\varepsilon}_{eq}$ and the structure diameter:

$$v_{maxfli} = 0.9 d \dot{\varepsilon}_{eq} \tag{5}$$

, with $\dot{\varepsilon}_{eq}$ equal to 10^{-2} [s^{-1}]. Based on experimental and full-scale work Huang et al. (2007) define an estimate of the maximum velocity as:

$$v_{maxfli,n} = \frac{D f_n}{e^{-\frac{20h}{D \ln\left(\frac{K_n}{Eh}\right)}}} \tag{6}$$

, with E the Young's modulus of ice [Pa], and K_n the stiffness used in a single-degree-of-

freedom representation of mode *n* [N/m]. Palmer (2010) suggests a velocity range estimate based on:

$$v_{fli,n} = \alpha f_n h \tag{7}$$

, with α between 0.01 and 0.4. Application of these four approaches to the structures considered gives the estimates for the maximum velocity at which lock-in can develop shown in Table 5. For the Huang approach we have chosen a range of *E* of 1 GPa up to 5 GPa (Timco and Weeks, 2010)

Table 5. Estimates of maximum ice drift velocity for frequency lock-in based on analytical approaches.

Structure:	ISO19906 Eq. (4)	Guo (2013) Eq. (5)	Huang et al. (2007) Eq. (6)	Palmer et al. (2010) Eq. (7)
Norströmsgrund lighthouse	0.156	0.0675	0 – 3.98	0.026 - 1.04
Monopod MDP-1	0.1392	0.016	0.01 – 0.45	0.011 - 0.464
OWT mode 1	0.014	0.054	0.68 – 0.93	0.001 - 0.036
OWT mode 2	0.035	0.054	1.86 – 2.57	0.0025 - 0.1

The obtained results are discussed in Section 5 in comparison to the numerical approach applied in the following Section.

APPLICATION OF A NUMERICAL APPROACH

In this section we analyze the development of frequency lock-in for the different structures on the basis of numerical simulations with a recently developed numerical model (Hendrikse and Metrikine, 2016).

Model Input Parameters

The model requires eight input parameters to define the ice. Reference data from ice action on a rigid structure is used to define these parameters. As the ice behavior when crushing against a rigid structure is not influenced by structural motion pure ice related input parameters can be obtained. For flexible structures, such as analyzed in this paper, the interaction between ice and structure may lead to intermittent crushing or frequency lock-in in which case the data reflect the interaction rather than pure ice behavior. Only in the continuous brittle crushing range at high ice drift velocities is the behavior more or less similar for both flexible and rigid structures.

We use the best match currently available to Baltic Sea data derived from the observations on the Norströmsgrund lighthouse (Ice Induced Vibrations JIP, 2011). Seven of the input parameters used for simulations are given in Table 6 for reproducibility of the results presented in this Section. It is worth commenting on the two velocities used as model input. The value for v_{trans} is the velocity at which a transition from ductile to brittle ice behavior occurs in the model. The value of $v_{ref,high}$ is a reference velocity above which the ice fails in a

completely brittle manner in continuous brittle crushing on a rigid structure. For velocities above this reference the mean global load and standard deviation are approximately constant as seen in the experiments by Sodhi and Morris (1984).

The remaining input parameter is the reference mean load level during continuous brittle crushing. This parameter is chosen such that the maximum simulated load levels during continuous brittle crushing correspond roughly to the load levels shown in Table 3. Table 7 shows the mean global ice load, maximum global ice load, and the amplitude during continuous brittle crushing as obtained from numerical simulation. For the monopod the ratio between amplitude and mean is much higher compared to the other structures as a result of the smaller ratio between structure diameter and ice thickness following the experimental results by Sodhi and Morris (1984).

Further discussion of the approach and definition of the parameters can be found in Hendrikse (2017). Simulations presented here were run for 100 cycles of oscillation of which the first 50 cycles were disregarded for the analysis to remove transient effects.

Table 6. Input parameters defining the ice behavior in the numerical model. For a detailed explanation see Hendrikse (2017).

Model input parameter	Magnitude
$v_{ref,high}$:	0.1 m/s
$f_{ref,peak}$:	20 Hz
v_{trans}	0.001 m/s
$F_{ref,max}/F_{ref,mean}$	5
$F_{ref,std}/F_{ref,mean}$	0.1
$F_{ref,mean,2}/F_{ref,mean}$	3
$T_{ref,peak}$	60 s

Table 7. Simulated global loads during continuous brittle crushing at high ice drift velocities for different load scenarios.

Structure and load scenario	Mean global load [MN]	Max global load [MN]	Amplitude	Amplitude / Mean [%]
Norströmsgrund lighthouse				
Load scenario 1	4.20	5.90	1.70	40%
Load scenario 2	5.90	8.30	2.40	41%
Load scenario 3	7.60	11.0	3.40	45%
Monopod MDP-1				
Load scenario 1	0.50	0.97	0.47	94%
Load scenario 2	0.71	1.30	0.59	83%
Load scenario 3	0.91	1.70	0.79	87%
Offshore wind turbine				

Load scenario 1	1.35	2.02	0.67	50%
Load scenario 2	1.90	2.80	0.90	47%
Load scenario 3	2.44	3.60	1.20	49%

Simulation Results

Simulation results for the Norströmsgrund lighthouse and the MDP-1 monopod are shown in Figure 2. The relation between the ice velocity and the maximum structural velocity is shown. The frequency lock-in range is given by the points which follow the relationship (Toyama et al., 1983):

$$v_{s,max} = \beta v_{ice} \tag{8}$$

, with $v_{s,max}$ the maximum structural velocity [m/s], and β a factor between 1.0 and 1.5.

The model predicts frequency lock-in for the Norströmsgrund lighthouse in the range of 0.02 m/s up to 0.09 m/s for the load scenarios considered. For the MDP-1 monopod frequency lock-in is predicted to occur between 0.02 and 0.06 m/s. It is seen that for higher load levels, corresponding to higher numbers of load scenario, the range where frequency lock-in is predicted to occur shifts to higher velocities. More energy is introduced by the ice at higher load levels resulting in this shift to higher velocities. For details see Hendrikse (2017).

Results for the first four modes of the offshore wind turbine are presented in Figure 3. Modes 3 and 4 show no frequency lock-in in any of the load scenarios considered. Mode 2 shows the largest range of frequency lock-in between 0.06 m/s and 0.11 m/s for the defined load scenarios. Mode 1 shows a transition in interaction between 0.04 m/s and 0.07 m/s for the considered load scenarios, but no pure frequency lock-in signal is obtained.

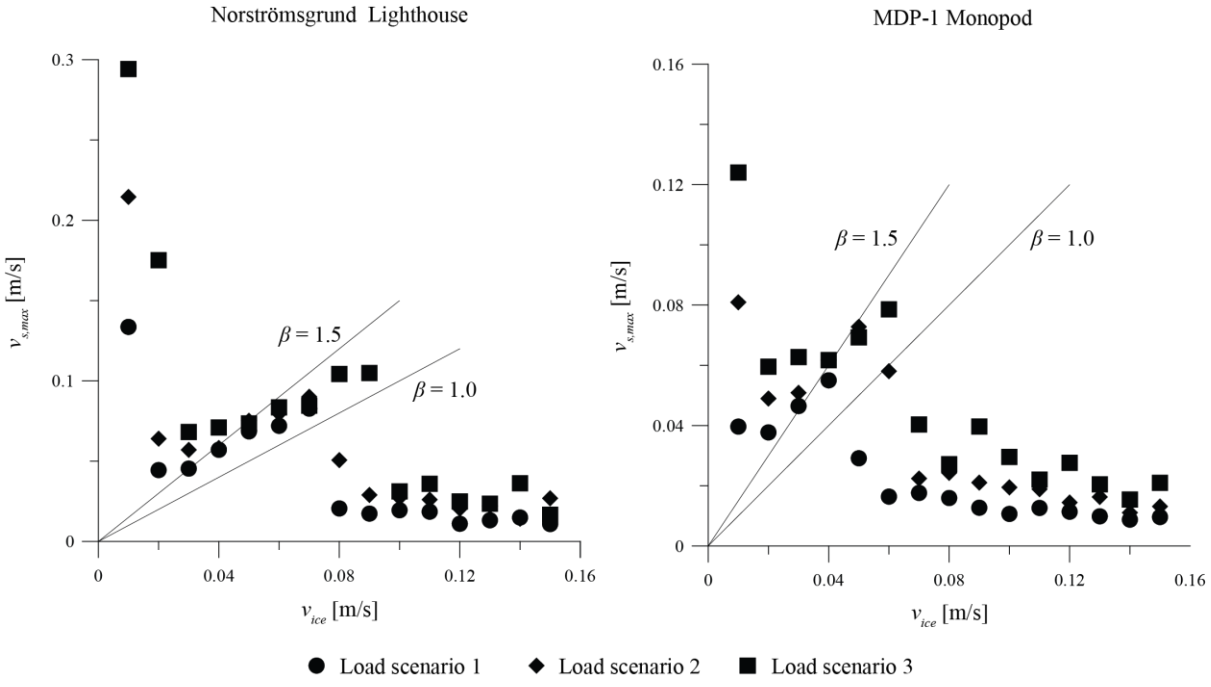

Figure 2. Left: Simulated dependence of maximum structural velocity on ice drift velocity for the Norströmsgrund lighthouse. Frequency lock-in is predicted to occur between 0.02 m/s and 0.09 m/s for the considered load scenarios. Right: Simulated dependence of maximum

structural velocity on ice drift velocity for the MDP-1 monopod. Frequency lock-in is predicted to occur between 0.02 m/s and 0.06 m/s for the different load scenarios considered. The solid lines represent a ratio of 1.0 and 1.5.

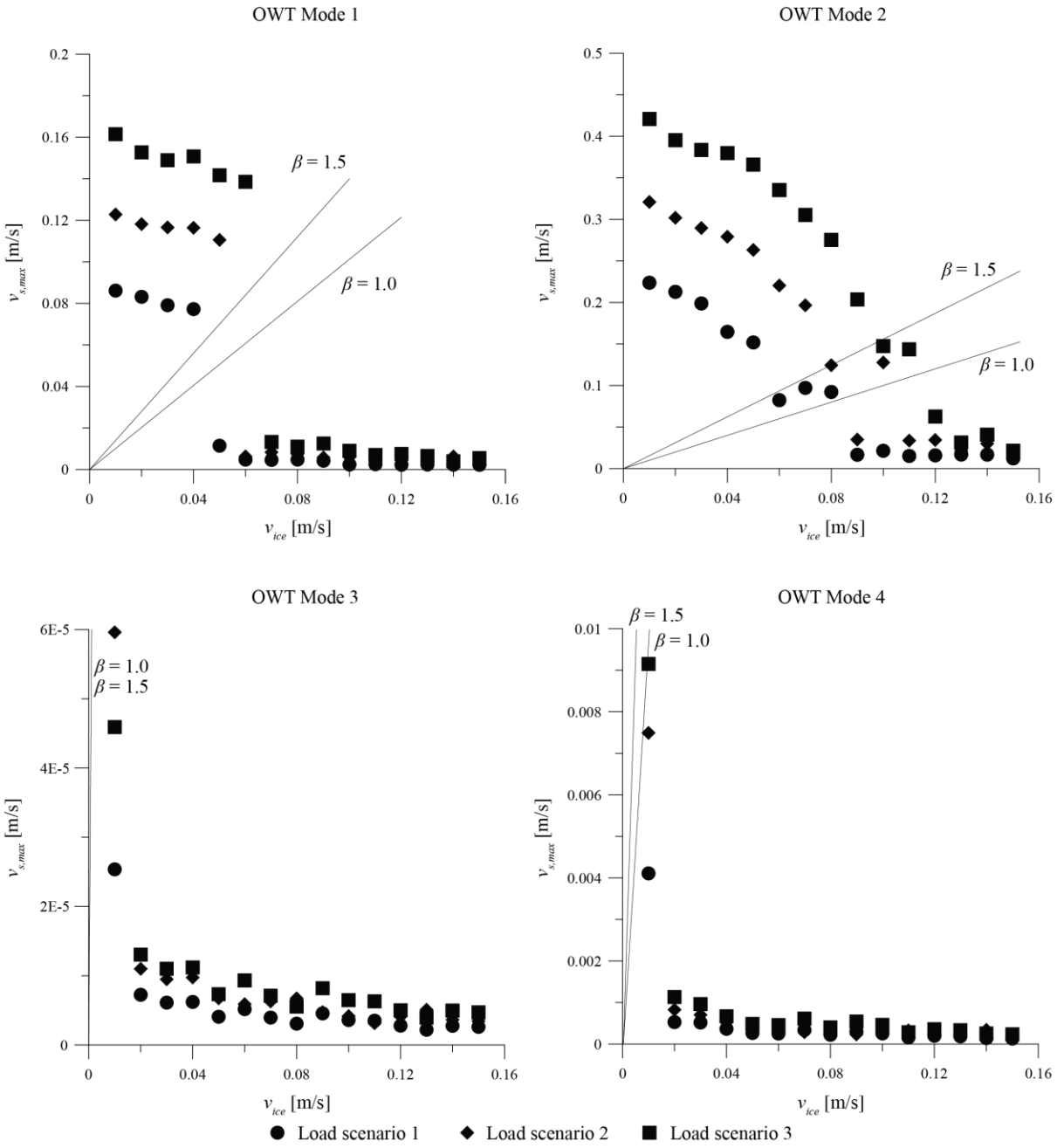

Figure 3. Simulated dependence of maximum structural velocity on ice drift velocity for the four modes of the offshore wind turbine. Modes 3 and 4 show no lock-in in any of the load scenarios. Mode 1 shows a transition in behavior in the range of 0.04 m/s up to 0.06 m/s, but no frequency lock-in is obtained. Mode 2 shows frequency lock-in between 0.06 m/s and 0.11 m/s for the different load scenarios considered. The solid lines represent a ratio of 1.0 and 1.5.

DISCUSSION

Modes Susceptible to Frequency Lock-in

With respect to the prediction of modes susceptible to frequency lock-in the analytical formula in ISO19906 (Eq. (2)) and the numerical approach used in Section 4 give the same results. Despite the fact that Eq. (2) does not reflect our current theoretical understanding of the interaction (Hendrikse, 2017) it gives a reasonable first indication of the susceptibility of a mode to frequency lock-in. Care must be taken with respect to the empirical parameter θ which incorporates effects of structure width and ice properties on the energy input from the ice and might not always be conservative.

Prediction of Ice Drift Velocities at which Frequency Lock-in Develops for Existing Structures

The predictions of the maximum velocity, or range of velocities, for frequency lock-in on the basis of the different estimation formulas (Eq. (3-6)) show a large scatter as illustrated in Figure 4. For the Norströmsgrund lighthouse only the formula used in ISO19906 predicts a reasonable upper bound estimate, but this is perhaps not surprising as the lighthouse were studied extensively as a basis for the standard. For the Monopod all formulas significantly over predict the maximum velocity compared to the observed velocity range, except for the estimation formula by Guo (2013) which results a value lower than the actual observations. None of the estimation formulas considered here gives a good estimate for the maximum velocities which could be used as input in Eq. (1) for design.

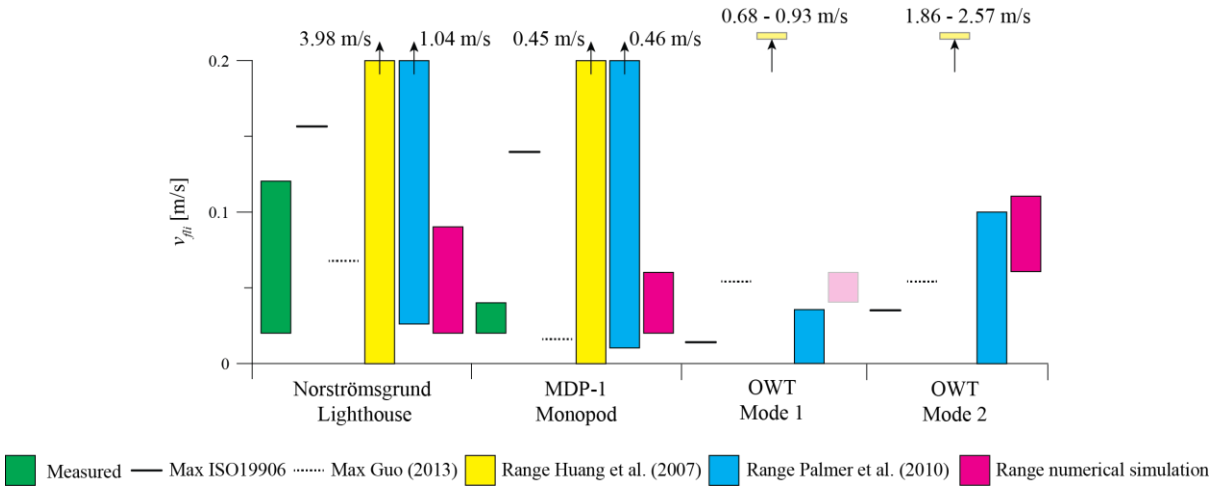

Figure 4. Summary of results for the predicted frequency lock-in velocity range or max velocity. For mode 1 of the offshore wind turbine the simulated possible range of frequency lock-in based on the behaviour transition illustrated in Figure 3 is shown.

The method using the numerical simulation model shows more consistent results for the lighthouse and the monopod as shown in Figure 4. The over prediction of the maximum velocity for the Monopod could be a result of the assumption of a too high global ice load in load scenarios 2 and 3. Load scenario one gives the best match with a range between 0.02 m/s and 0.04 m/s. There is not enough load data available to compare between simulated load levels and real load levels which have resulted in frequency lock-in of the monopod.

For the Norströmsgrund lighthouse a lower maximum is predicted in the considered ice load

conditions. The load scenarios considered yield high load values compared to those actually measured on the lighthouse and therefore a similar over prediction of the maximum velocity as for the monopod would be expected. An effect which is not included here which is very relevant for stiffer structures, such as the Norströmsgrund lighthouse, is the importance of initial conditions. The interaction problem is to some extent sensitive to initial conditions as frequency lock-in may not be possible to develop from the initial equilibrium position, but the limit cycle can be reached with favorable initial conditions. At velocities above the range predicted as shown in Figure 4 short periods of frequency lock-in sometimes develop. An example is shown for the Norströmsgrund lighthouse in load scenario 2 at 0.12 m/s in Figure 5. Frequency lock-in has often been observed to develop for short amounts of time on the lighthouse (Bjerkås et al., 2014). This could indicate that the majority of events measured was actually driven by the initial conditions. A more detailed study into the effect of initial conditions on the predictions is ongoing.

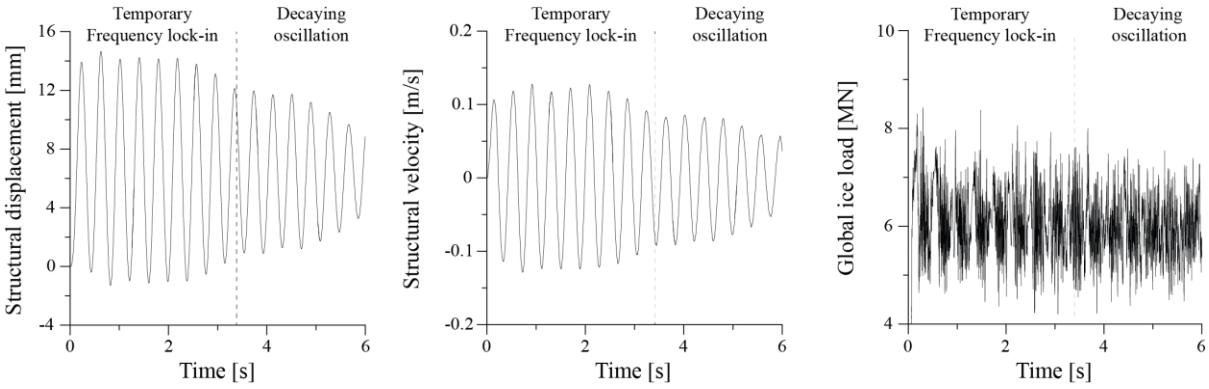

Figure 5. Short duration frequency lock-in of the Norströmsgrund lighthouse in load scenario 2 at a high velocity (0.12 m/s) as a result of initial conditions. Frequency lock-in is sustained for 7 cycles before the oscillations start to decay and the interaction is lost.

A degree of conservativeness has to be applied when using the maximum velocity from model simulations as input for simplified design approaches to account for the effect of initial conditions. For FLS predictions the effect is relatively small as initial condition driven frequency lock-in is generally not stable for long periods of time and changing ice conditions.

Prediction of Ice Drift Velocities at which Frequency Lock-in Dvelops for the Offshore Wind Turbine

Results for the offshore wind turbine shown in Figure 4 illustrate that in general the estimation formulas predict frequency lock-in at much lower velocities than for the lighthouse and the monopod, with the exception of the approach by Guo (2013). This is surprising as comparison between the second mode of the offshore wind turbine and the first mode of the lighthouse shows that the offshore wind turbine has lower damping and a lower natural frequency which on the basis of experiments would suggest frequency lock-in at higher velocities (Huang et al., 2007).

Based on the numerical approach the offshore wind turbine is shown to be susceptible to frequency lock-in primarily in the second mode. For the different load scenarios considered the range even extends to values higher than those simulated for the lighthouse. This is an important observation as it is often suggested in literature that sustained frequency lock-in cannot develop above 0.1 m/s (ISO19906, 2010). Full-scale observations on channel markers

and model-scale experimental observations suggest that such theoretical limit does not exist and support the model predictions (Nordlund et al., 1988; Huang et al., 2007). Recent theoretical development (Hendrikse, 2017) also suggests that no such limit exists and that for structures with low damping in severe ice conditions the maximum velocity could increase significantly above 0.1 m/s.

With respect to the first mode it is observed that the natural period is so large such that during a single cycle of interaction a long time occurs during which the contact area between ice and structure increases in the model. This sometimes results in a large increase in the resistance of the ice. As a result the structure experiences a mix of frequency lock-in and intermittent crushing like behavior as illustrated in Figure 5 for load scenario 2 and a velocity of 0.04 m/s. There are no data available to validate this type of behavior. Experiments aimed at investigating frequency lock-in for structures with low natural frequencies are required.

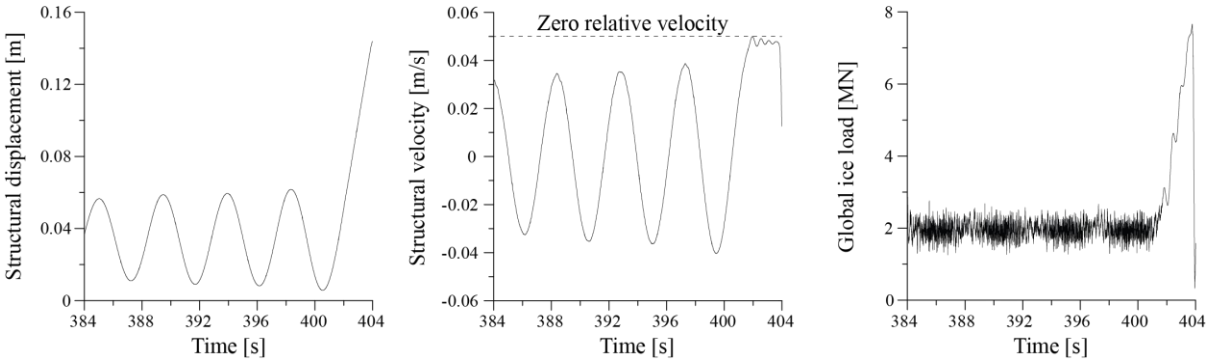

Figure 5 Simulated mixed frequency lock-in and intermittent crushing interaction at 0.04 m/s for load scenario 2 for mode 1 of the offshore wind turbine. A single mixed cycle is shown. At the moment when the amplitude of oscillation reaches close to zero relative velocity the ice resistance increases enough as a result of ductile ice behavior to prevent the structure from moving back and the oscillation pattern is interrupted by a typical intermittent crushing type of interaction.

CONCLUSION

The estimation of the susceptibility of structural modes to frequency lock-in and the range of ice drift velocities for which frequency lock-in can develop in given ice conditions has been studied. Three structures have been analyzed, being the Norströmsgrund lighthouse, MDP-1 monopod, and an offshore wind turbine designed for southern Baltic Sea ice conditions. The analysis has been conducted on the basis of both existing estimation formulas from literature and numerical modelling of the interaction with a recently developed model.

With respect to the prediction of the susceptibility of modes to frequency lock-in both the estimation formulas and the numerical approach show to be consistent with observations on the existing structures. The first mode of the lighthouse and monopod are correctly predicted to be susceptible to frequency lock-in. For the offshore wind turbine it has been found that the first and second mode are susceptible to frequency lock-in in the defined ice conditions based on both the estimation formulas and the numerical approach.

The estimation formulas from literature show a significant scatter in the predictions for the maximum velocity and velocity range at which frequency lock-in can develop. None of the formulas matches the observations of the lighthouse and monopod and they can therefore not

be applied for simplified design approaches.

The numerical method shows results consistent with the observations of the lighthouse and monopod. A good estimate for the maximum velocity at which frequency lock-in can develop can be obtained with the numerical method allowing for a simplified design approach based on characteristics of the structural motion during frequency lock-in. Care should be taken to include a degree of safety in the estimate to account for the effect of initial conditions on the maximum predicted velocity at which frequency lock-in develops.

The results obtained with the numerical approach show that frequency lock-in is most likely to develop in the second mode of the offshore wind turbine considered. For moderate ice climates in the southern Baltic Sea, with ice thickness not exceeding 0.5 m and an ice load level given by a C_R value of 1.0, the example of the OWT structure calculated shows maximum ice drift velocities for frequency lock-in of 0.06 m/s for the first mode (in the region of 0.25Hz) and 0.1 m/s for the second mode (around 1.0Hz). These values can be used as an indication for conceptual design purposes, but validation with an interaction model is highly recommended at later design stages.

ACKNOWLEDGEMENTS

The authors acknowledge the support from the SAMCoT CRI through the Research Council of Norway and all the SAMCoT partners. Thanks to Chris Keijdener for his input during revision of the paper.

REFERENCES

Bjerkås, M., Alsos, H.S., & Wåsjø, K., 2014. Estimates of the number of vibration cycles from frequency locked-in ice loads. In *Proceedings of the ASME 2014 33rd International Conference on Ocean, Offshore and Arctic Engineering*, OMAE2014-23134.

Blenkarn, K. A., 1970. Measurements and analysis of ice forces on Cook Inlet structures. In *Proceedings of the Second Annual Offshore Technology Conference*, volume II, pp.365–378.

Gravesen, H., & Kärnä, T., 2009. Ice loads for offshore wind tutbines in Southern Baltic Sea. In *Proceedings of the 20th International Conference on Port and Ocean Engineering under Atctic Conditions*, POAC09-3.

Guo, F., 2012. Reanalysis of Ice Induced Steady State Vibration from an Engineering Perspective. In *Proceedings of the 21st IAHR International Symposium on Ice*, pp.1023-1034.

Guo, F., 2013. Analysis of the key parameters in ice induced frequency lock-in. In *Proceedings of the 22nd International Conference on Port and Ocean Engineering under Arctic Conditions*, POAC13-33.

Hendrikse, H., 2017. *Ice-induced vibrations of vertically sided offshore structures.* Ph.D. Delft: Delft University of Technology.

Hendrikse, H., & Metrikine, A., 2016. Ice-induced vibrations and ice buckling. *Cold Regions Science and Technology*, 121, pp.100-107.

Huang, Y., Shi, Q., & Song, A., 2007. Model test study of the interaction between ice and a compliant vertical narrow structure. *Cold Regions Science and Technology*, 49, pp.151-160.

Ice Induced Vibrations JIP, 2011. *Full-scale data analyses of frequency lock-in,OO-11179-1.2.2*, Norway: Dr.techn.OlavOlsen.

ISO19906 (2010). *Petroleum and natural gas industries – arctic offshore structures*.

Izumiyama, K., Irani, M.B., and Timco, G.W., 1994. Influence of compliance of structure on ice load. In *Proceedings of the 12th IAHR International Symposium on Ice*, volume 1, pp.229–238.

Jefferies, M.G., & Wright, W.H., 1988. Dynamic response of 'Molikpaq' to ice-structure interaction. In *Proceedings of the Seventh International Conference on Offshore Mechanics and Arctic Engineering*, volume 4, pp.201–220.

Nordlund, O.P., Kärnä, T., & Järvinen, E., 1988. Measurements of ice-induced vibrations of channel markers. In *Proceedings of the IAHR 9th International Symposium on Ice*, volume 1., pp.537-548.

Palmer, A., Yue, Q., & Guo, F., 2010. Ice-induced vibrations and scaling. *Cold Regions Science and Technology*, 60, pp.189-192.

Peyton, H.R., 1968. Sea ice forces. In *Ice Pressures Against Structures, compiled by L. Gold and G.Williams, NRC Techn.Memo No. 92*.

Saeki, H., Hirayama, K., Kawasaki, T., Akagawa, S., Kato, K., Kamesaki, K., Saka, K., & Kurokawa, A., 1996. JOIA project of study on ice load. In *Proceedings of the 13th IAHR International Symposiumon Ice*, volume 1, pp.17–27.

Schwarz, J., & Jochmann, P., 2001. Ice force measurements within the LOLEIF-project. In *Proceedings of the 16th International Conference on Port and Ocean Engineering under Arctic Conditions*, volume 2, pp.669–682.

Singh, S. K., Timco, G.W., Frederking, R.M.W., & Jordaan, I.J., 1990. Tests of ice crushing on a flexible structure. In *Proceedings of the Ninth Offshore Mechanics and Arcitc Engineering Symposium*, volume 4, pp.89–94.

Sodhi, D. S., & Morris, C. E., 1984. Ice forces on rigid, vertical, cylindrical structures. *Report 84-33*, US Army Cold Regions Research and Engineering Laboratory.

Timco, G.W., & Weeks, W.F., 2010. A review of the engineering properties of sea ice. *Cold Regions Science and Technology*, 60, pp.107-129.

Toyama, y., Sensu, T., Minami, M., & Yashima, N., 1983. Model tests on ice-induced self-excited vibration of cylindrical structures. In *Proceedings of the 7th International Conference on Port and Ocean Engineering under Arctic Conditions*, pp.834-844.

Yue, Q., Bi, X., Zhang, X., & Kärnä, T., 2002. Dynamic ice forces caused by crushing failure. In: Ice in the Environment, *Proceedings of the 16th IAHR International Symposium on Ice*, pp.231-237.